THE STATIC STIFFNESS OF THE INTERFERENCE SHRINK-FITTED JOINTS

الجساءة الاستاتيكية لوصلات التداخل بالانكمـــاش

by

Ibrahim Elewa* and Robert Thornley**

* Lecturer, Industrial Production Engineering Department, Mansoura University, Mansoura, Egypt
** Professor, Department of Mechanical & Production Engineering, Aston University, UK.

ة ـ الهدف الرئيسى لهذا البحث هو دراسة تأثير كل من حجم ، ودرجة خشونة ، وقيمة التداخل سين سطحى عضوى جلب ذات تداخل بالانكماش على الأداء الاستاتيكى لها . ولقد انصب اهتمام الأبحـــاث السابقة لدراسة قوة تحمل هذه الجلب تحت تأثير الأحمال الاستاتيكية دون اعطاء أى اعتبار للحـــالات التى تتعرض فيها للأحمال الديناميكية . أن الأداء الديناميكى لماكينات التشغيل يعتمد الى حـــد كبير على الأداء الديناميكى للوصلات المختلفة المكونة لهذه الماكينات أن هناك كثيرا مـــن تطبيقات التى تستخدم فيها جلب ذات تداخل بالانكماش ومنها على سبيل المثال المخركات وماكينـــات تشغيل والتى يكون أداءها الديناميكى من الاهمية بمكان لتحديد كفائتها الانتاجية . لذا كانـــت دراسة الأداء الاستاتيكى والديناميكى لجلب ذات تداخل بالانكماش أمرا فى غاية الاهمية .

SUMMARY The main objective of the work is to investigate the effect of size, surface roughness and the interference value on the static stiffness of shrink-fitted joints.

Most of the previous research has been concerned with the joint holding load under static conditions without consideration to many of the applications in which the joints are exposed to dynamic loading. The dynamic performance of a machine tool is greatly affected by the collected response of its joints. In many applications in which shrink fitted joints are used, such as engines and machine tools, their dynamic characteristics can be an important factor in deciding the overall performance of the machine. Hence, studying the joints stiffness characteristics under static and dynamic conditions is of great importance.

INTRODUCTION

In practice, joints are in most cases subjected to a system of loads such that normal and shear forces are transmitted by the joint interface. The main requirements for machine tool joints are stiffness and wear resistance. In machining operations the accuracy is affected by the normal and shear displacements in the different machine joints, such as rotary table, dead stop, cutter-heads, slides and also the turre in precision machine tools. In high precision machine tools operating with very low cutting forces, the machining accuracy is also affected by the shear deformations in a contact joint due to dynamic forces developed during the operation. The conditions under which such joints operate should ensure that any deformation must be limited to the elastic range. In the case of fixed joints, the static and dynamic stiffnesses are especially important factors , as they determine the dynamic behaviour of the machine tool.

A considerable amount of the work in the past four decades has been directed towards investigating the mechanism within the joint interfaces . The early investigations date as far back as 1699 to Amonton's laws of friction, their verification by Couloumb and their later development by Bowden and Tabor [1].

THE TANGENTIAL STIFFNESS OF THE JOINT

In many practical configurations joints are subjected to tangential loading. The information on stiffness characteristics of machine tool joints in the tangential direction is limited when compared to that of the normal direction. The reason may be attributed to the difficulty in arriving at reliable predictions due to the constant deterioration caused by fretting, corrosion and its irreversible behaviour. However, the calculations for the joints failure in the tangential direction are normally carried out on the basis of the coefficient of friction, but this may prove unsatisfactory in some cases beause the loads may exceed the elastic limit causing irreversible displacements to occur before the joint fails. It is necessary to design the joint in such a way that the shear deformations remain below the plastic limit.

Kirsanova [2] has been one of the early investigators to study the characteristics of joint surfaces loaded in the tangential direction. The test specimens were made of grey cast iron with large contact areas (225cm^2). The results show that for repeated loads which do not exceed the first loading limit, the displacements are also limited to the elastic range. It has also been observed that at the elastic limit, the ratio between the shear stress and the normal stress has a constant value over the measured pressure range (1 to 15 kp/cm^2). This ratio is approximately half the static coefficient of friction.

Masumo et al. [3] has also investigated the shear stiffness of bolted joints using steel and cast iron specimens and interface pressures of 100 and 200 kg/cm^2. They report that the horizontal displacements of the joint surfaces are larger than for the equivalent solid specimen and that it is due to the sum of the elastic displacement and the micro-sliding between the joint surfaces. The results show that the joint stiffness has a value of about 70 to 90% compared to the stiffness of the equivalent solid in spite of the very high preload.

The results obtained by Back et al. [4,5,6] show that, after the initial application of the shear pressure, a large amount of permanent deformation is observed. They consider this deformation to represent the plastic shear deflection of the asperities. After the good repeatability if the shear pressure is kept equal to or below the first maximum loading.

Later, Shoukry and Thornley [7] have carried out theoretical estimations for normal and tangential stiffness of machine surfaces using a mathematical model. The conditions of the surface roughness and flatness deviations on the joint surface are included in the model. Their results are in agreement with the Back results.

THE ELASTIC DEFORMATION AND MICRO-SLIP

When the joint surfaces are subjected to a tangential load even smaller than the frictional forces, a micro-slip can be sensed on the joint. From the standpoint of a structural design of a machine tool this micro-slip is as important as the tangential stiffness [8].

Goodman et al. [9] reported that, when a sphere is held between parallel flat surfaces by means of a constant clamping pressure and then subjected to a cyclic tangential displacement parallel to the flats, energy is dissipated at the contact. This occurs even when the maximum tangential force is less than the friction forces. Goodman suggests that, during the application of the normal load, there is no relative slip of the points in contact.

Masumo et al. [10] suggests that the residual displacement is due to the micro-slip between the joint surfaces or the microplastic deformation on the joint surface asperities.

The surface roughness of the joint has significant effect on the tangential

stiffness and micro-sliding. The micro-sliding gradually decreases with the roughening of the surface, while the tangential stiffness increases with decreasing the surface roughness [10].

SPECIMEN PREPARATION AND TEST PROCEDURES

The method adopted to produce the shrink-fitted joint consisted of heating the ring in an induction oven and cooling the shaft using liquid nitrogen. The shaft and ring were then assembled together using a special fixture adopted to a bench drilling machine. Half the specimens were tested statically and the other half dynamically.

The specimens used were manufactured from mild steel bar (ENIA) as shown in Figure 1. The manufacturing process has a significant influence on the type of surface finish obtained. Hence, it was necessary to change the process type and process parameters to obtain various levels and types of finish on the specimens used, (see Table 1).

MEASUREMENT TECHNIQUES

Dimensional Measurements

The outer diameter of the shaft and the inner diameter of the ring were measured using a Universal Measuring Machine model (Mu 214 B). Six readings were taken axially for each shaft or ring with the average value taken as the effective diameter. (Machine sensitivity + 1 μ m). A spherical-ended feeler of 6 mm diameter was used for diameter measurement to avoid including the specimen roughness in the measurement.

The straightness of the shafts and rings was measured using a Taylor Hobson Talylin 1, by taking different traces along the length of the specimen. The specimen's out-of-roundness was assessed using a Taylor Hobson Talyrond Model (1). A number of traces were recorded for each diameter at constant intervals along the specimen's height.

Surface Finish Measurement

The centre line average CLA of the specimens was determined using a Taylor Hobson Talysurf 4. The stylus was positioned to move along the specimens which were held in a vee-block to obtain the (CLA) value across the lay. The mean value of (CLA) was taken as the average of ten readings. A mean value of the peak to valley height (H_t) was calculated from a trace taken across the lay for every specimen.

The talysurf level potentiometer was set above and below the mean line to measure the percentage of the bearing area at different roughness levels. Two traces across the lay were taken to evaluate the B.A., with the high spot count recorded at each potentiometer level. For each specimen ten traces were taken at the mean line from which the average wave length was calculated as the quotient of dividing the stroke length by the number of spots.

Joint Assembly

A pair consisting of a shaft and ring of almost the same surface finish (CLA) were assembled as joints of different values of interference, fulfilling the following conditions.

a) To provide adequate interference to ensure satisfactory strength for the finished assembly.

b) To keep the stresses resulting from the fit below the level of the material's allowable stress.

c). To ensure that the amount of heating and cooling of the rings and shafts respectively would provide an adequate clearance for assembly .

Shrink-Fitting Procedure

The specimens were first degreased and dried, after which the shafts were loaded into the fixture and lowered into the Liquid Nitrogen bath. The rings were placed inside an induction oven for a predetermined time and temperature. A jig was specially designed to ensure the best possible alignment during assembly of the joint. The shafts were clamped inside a jig and fitted to the spindle of an accurate bench drill. The heated rings were placed on a floating table (Figure 2) located on the drill base. The axial movement of the machine spindle was used to position the shaft inside the ring to a predetermined depth. The assembly was left in this position for a few seconds to form the joint. The joint was then left to cool down to room temperature.

Experimental Investigation

A special purpose rig for the static and dynamic testing of specimens was designed and manufactured as shown in Figure 3.

As shown in Figure 4 the shaft was connected to the hydraulic vibrator through a mounting fixture, whilst the ring was in contact with a load cell (Kistler 9051) placed on the ring base.

The joint was loaded with a predetermined loading increment and the shear compliance measured using an electronic comparator (Model 1) before removing the load and measuring the amount of micro-slip.

The process was repeated by adding loading increments until the loading level was sufficiently high to cause gross-slip, which was considered to be the joint's static holding load.

Dynamic Testing

This series of tests was performed to study the effect of the dynamic loading on the stiffness of a shrink-fitted joint.

The joint was held in the experimental rig in the same way as for the static testing. The only exceptions were in preloading the ring with a constant load of 20 KN., as well as using the vibrator to induce varying levels of amplitude of vibration to the shaft (constant frequency of 25 Hz).

The joint was loaded incrementally and the amplitude of shear compliance measured at each loading level. The exciting force from the vibrator was measured using an impedance head (Kistler 11280), while the joint's deformation was measured using a displacement transducer (Wynne-Kerr B731 B).

At each load the amplitude of the exciting force and slip signal were recorded using a frequency response analyser (Solartron 1170).

Displacement Measuring System

The whole system of measurements of stiffness, hinges on the effective measurements of the displacement between the two mating surfaces in the tangential direction.

A metronin comparator, which was held in a special fixture underneath the shaft, was used to measure the displacement during loading and unloading for the static test. The signal from the comparator was passed through a charge amplifier, selecting the appropriate magnification on the recording unit.

Under dynamic testing conditions the displacements were measured using capacitive type pickups, provided with variable sensitivity ranges. The displacement probe was situated underneath the shaft and connected to the distance meter and power supply. The instrument displays the actual gap setting on a graduated scale and its output terminal was connected to the frequency analyser. The mains frequency noise was eliminated using a special tunable filter connected between the instrument and the fequency analyser. Provision was also made to monitor the output signal of the probe on an oscilloscope.

RESULTS AND DISCUSSION

Tangential Displacement

The Effect of Value of Interference

Figures 5 to 8 show the effect of the joint interference value on the amount of tangential displacement for both the statically and dynamically tested joints. The graphs are plotted for the total value of tangential displacement as the sum of the elastic displacement and the micro slip. The load-displacement relationship for the equivalent solid specimen is also included to provide a comprison with the tested joints.

The tangential displacement increases almost linearly with the applied tangential load during the loading cycles for the large interferencee values. From the figures it can be seen that the value of interference plays an important role in determining the amount of tangential displacement between the joint mating surfaces. A proportional decrease in the tangential displacement can be observed when increasing the joint interference value, until finally reaching a value almost equal to the tangential displacement of the equivalent solid specimen for all joint sizes. When the tangential load reaches a magnitude equivalent to the joint holding load, gross-slip or sliding occurs and the joint can no longer be considered a shrink-fitted joint. For small interference values the load-tangential displacement curve has proved to be non-linear. At end of the unloading cycle in which the applied load is incrementally decreased until reaching zero load, a permanent tagential displacement is observed. This can be taken to represent the amount of plastic deformation and micro-sliding that occurred in the joint mating surfaces.

The interference level has a significant effect in determining the amount of the joint micro-slip. There is an inverse proportionality between, the value of interference and the amount of micro-slip, which proves to be almost insignificant at high values of interference, as can be seen from Figures 9 to 12. Subsequent loading and unloading cycles produce good repeatability. The same value of applied load has to be reached to achieve the original tangential displacement before the start of the unloading cycle.

The type of hystersis loops observed for the case of shrink-fitted joints can be divided into two types, as shown in Figures 9 to 12. In the first type the loop is characterised by a repeatable loop of small width at all loads below the joint holding load for joints with large values of interference. The other type also has a repeatable loop, but it has a much larger width and mostly occurs for joints with small interference levels. The area enclosed by both types of loops is considered to be small compared with the materials having different mechanical properties.

The Effect of Surface Roughness

When taken sequentially, Figures 5 to 8 can show the effect of the joint surface

roughness on the amount of tangential displacement of the mating surfaces. To clarify the effects of the joint surfaces, the displacement of the equivalent solid specimen must be eliminated from the overall tangential displacement of the joints. It is also noticed that the elastic displacement of shrink-fitted joints during unloading is about 90% of the overall tangential displacement for large values of interference. Therefore, the elastic displacement can be taken to represent the tangential displacement of the shrink-fitted joints with a large value of interference, if the tangential load is less than the joint holding load.

For all joint sizes an increase in the joint surface roughness leads to a proportional increase in the amount of tangential displacement and micro-slip at the same loading level.

THE JOINT TANGENTIAL STIFFNESS UNDER STATIC AND DYNAMIC LOADING

The tangential stiffness for the shrink-fitted joints is estimated using the following equation:

$$K_S = \frac{F_S}{\delta_\beta \Lambda} \qquad N / um / mm^2$$

Figures 13 to 16 show the relationship between the tangential load and the value of static stiffness. The stiffness of the equivalent solid specimen is also included for comparison. It is clear from these figures that the value of interference plays an important role in determining the value of joint stiffness. At large joint interference value the tangential stiffness is between 75 to 93% of the equivalent solid specimen value. The relationship between the joint stiffness and the applied tangential load has proved to be almost linear for high interference values, while it deviates from linearity with decreasing the interference value. Some fluctuation in the joint stiffness is observed with increasing the tangential load. This can be explained by the occurrence of micro stick slip conditions between the contacting asperities. Under dynamic loading the amount of fluctuation in the tangential displacement is much more pronounced due to the repeated change in the loading direction, which can give rise to the amount of wear between the asperities.

The variation of the joint tangential stiffness is highly dependent on the surface roughness of the mating surface. It can be observed that under both static and dynamic loading, the stiffness increased with decreasing surface roughness for all joint sizes. The effect of changing the joint surface roughness is shown in Figures 13 to 16. The value of surface roughness plays an important part in determining the conditions and amount of the micro-slip and, consequently, the joint tangential stiffness. The amount of micro stick slip increases with increasing joint surface roughness.

CONCLUSIONS

1. The mean value of interference (δ_m) has a significant influence on the joint tangential displacement. The displacement decreases with increasing interference value, reaching a constant value nearly equal to the displacement of the equivalent solid speciment.
2. The relationship between the tangential displacement and the applied load proves to be linear for large interference values. However, it deviates from linearity for small values of interference.
3. The value of the joint tangential displacement and micro-slip increases with increasing surface roughness at the same interference level.
4. The elastic displacement of shrink-fitted joints after unloading is approximately 90% of the overall tangential displacement of the joints with large interference values. Hence, the elastic displacement can be considered equivalent to the tangential displacement up to the value of the joint holding load.

5. The hysteresis loops observed for shrink-fitted joints prove to be repeatable at all loading levels, while their width depends on the value of interference.

6. The tangential stiffness of shrink-fitted joints increases with increasing interference value and surface finish. It represents approximatelty 75 to 93% of the stiffness of the equivalent solid specimen for large interference values.

7. Under dynamic loading the amount of fluctustions in the tangential displacement is considerably more pronounced than the fluctuation observed under static loading.

NOMENCLATURE

δm	Mean value of interference on the diameter.
CLA	Centre line average on the surface profile.
H_t	Peak to valley height of the surface profile.
K^s	Tangential stiffness N/um / mm^2
F^s	Tangential load.
δ_B	The elastic shearing deformation between the joint surfaces.
A	The apparent contact area.
s	Tangential displacement um.
d	Joint nominal size.
E.S.S.	Equivalent solid specimen.

REFERENCES

1. DOWDEN F P and TABOR D., Friction and lubrication of solids. Oxford University Press, 1964.

2. KIRSANOVA V N., The shear compliance of flat joints. Machines and Tooling, 38, No. 7, 1967.

3. MASUKO M., ITO Y., and KOIZUMI T., Horizontal stiffness and microslip on a bolted joint subjected to repeated tangential static loads. JSME., Vol. 17, No. 113, 1974.

4. BACK N., Deformation in machine tool joints. PhD thesis. UMIST 1972.

5. BACK N., BURDEKIN M., and COWLEY A., Review of the research on fixed and sliding joints. Int. MTDR. Conf., 1972.

6. BURDEKIN M., COWLEY A., and BACK N., Experimental study of normal and shear characteristics of machined surfaces in contact. J. Mech. Eng. Science, Vol. 20, No. 3, 1978.

7. SHOUKRY S., and THORNLEY R H., Theoretical expressions for the normal and tangential stiffness of machine tool joints. Proc. of 22nd Int. MTDR. Conf., UMIST, 1981.

8. ITO Y., and MASUKO M., Experimental Study on the optimum interface pressure on a bolted joint. 12th MTDR. Conf. 1971.

9. GOODMAN L E., and BROWN C B., Energy dissipation in contact friction: Contact normal and cyclic tangential loading J. of Applied Mech., 1962.

10. MASUMO M., ITO Y., and FUJIMOTO C., Behaviour of the horizontal stiffness and the micro-sliding on the bolted joint under the normal preload. Int. MIDR. Conf., 1971.

TABLE I

Coding System

ST : Static Test
D : Dynamic Test

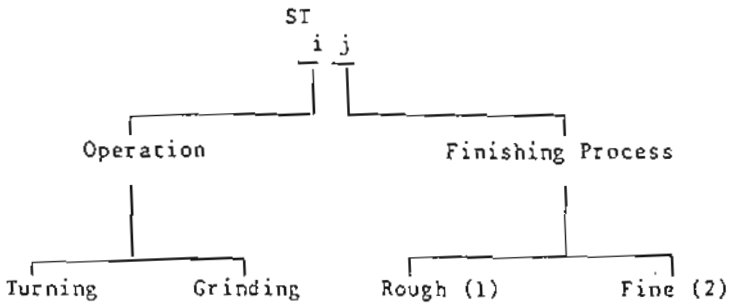

Size mm	Turning Code	Grinding Code
10	1	2
15	3	4
20	5	6

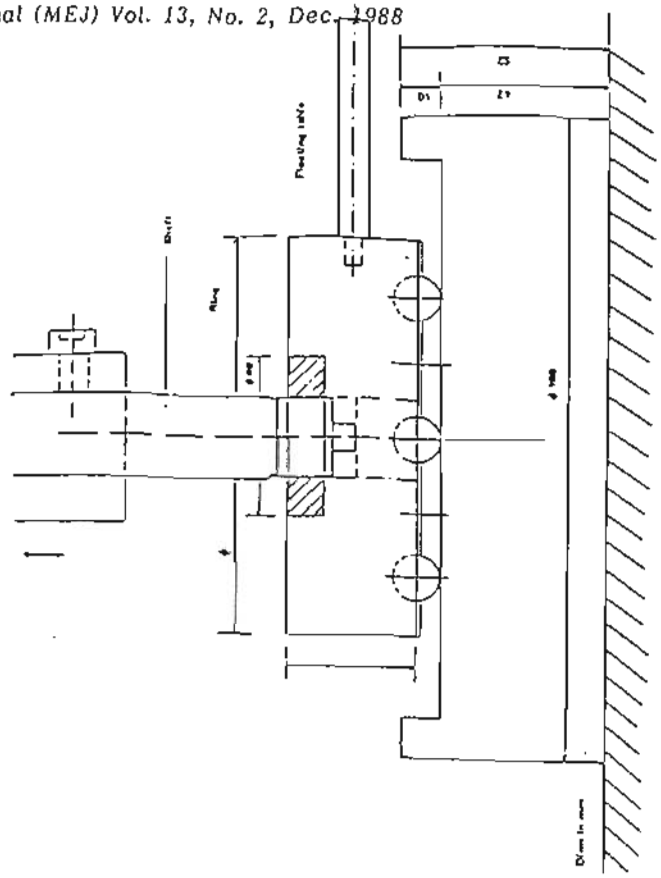

Fig.2 Shrink Fitting Arrangement

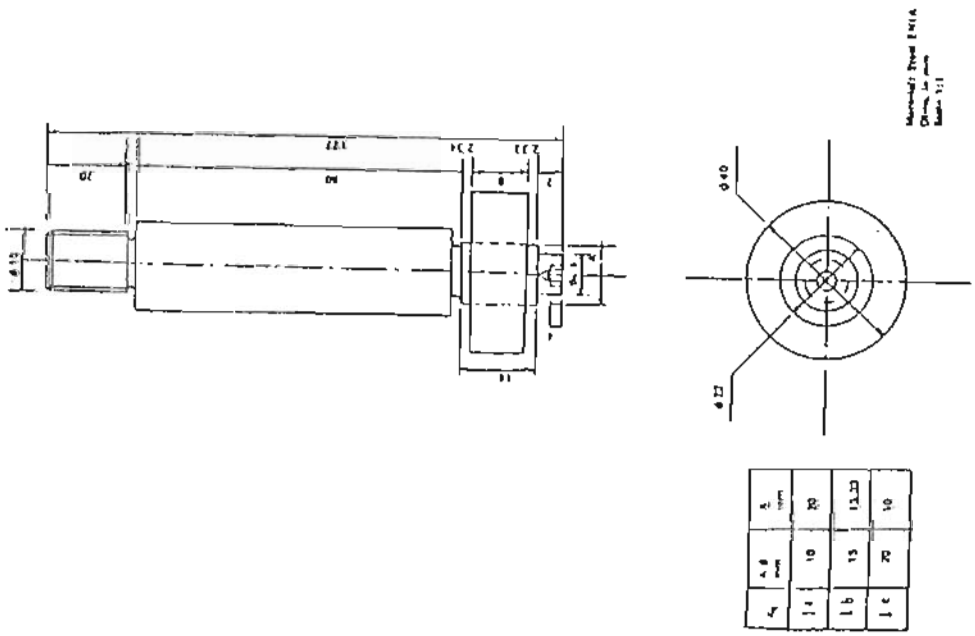

Fig.1 Test Specimen Dimensions

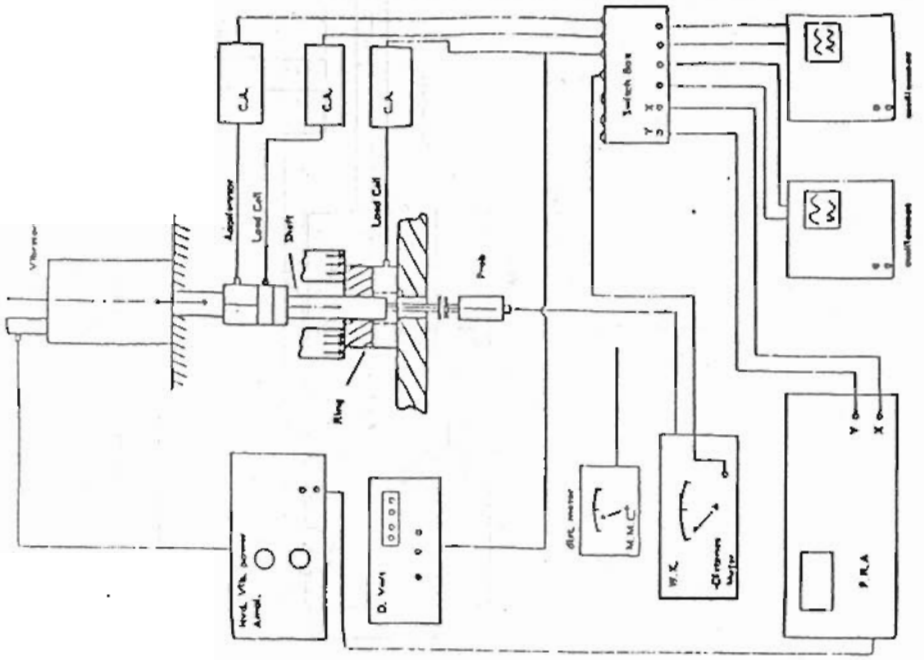

Fig.4 The testing system block diagram

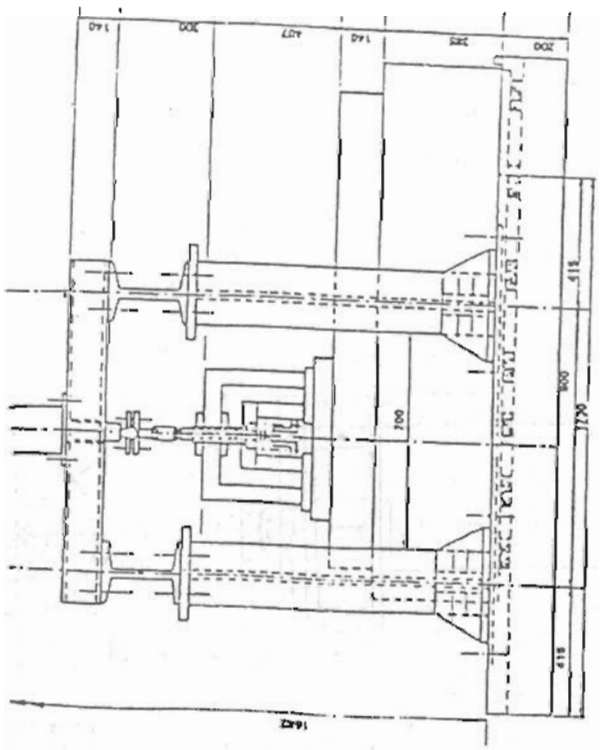

Fig.3 Schematic Diagram of the test rig.

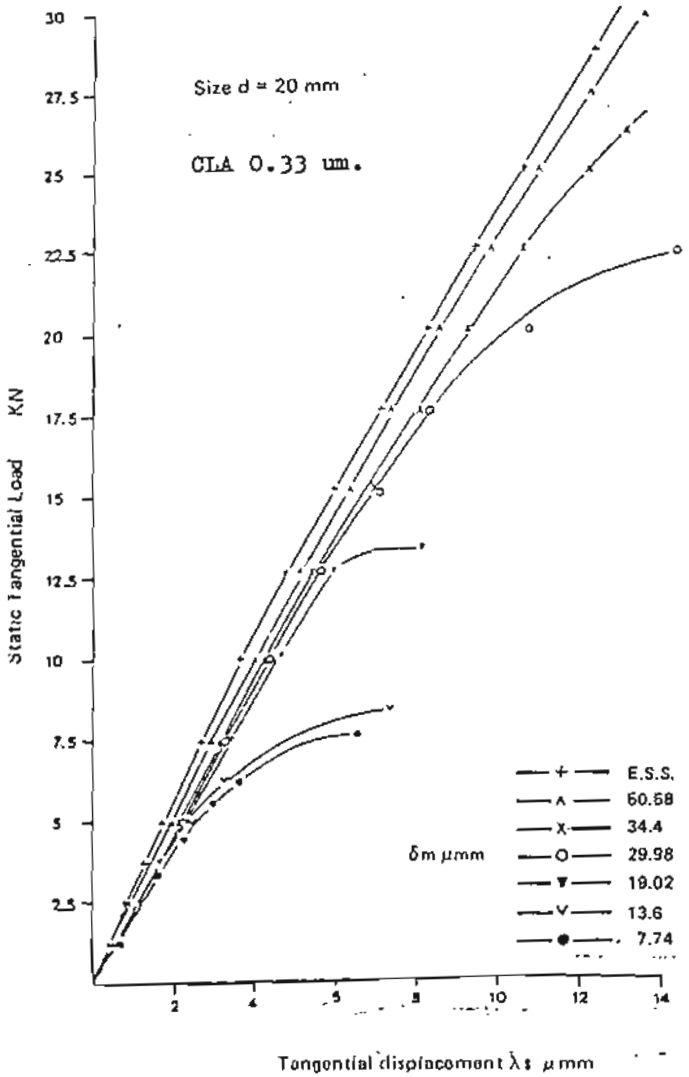

Fig 5 Effect of the interference value on λs of ST62 joints

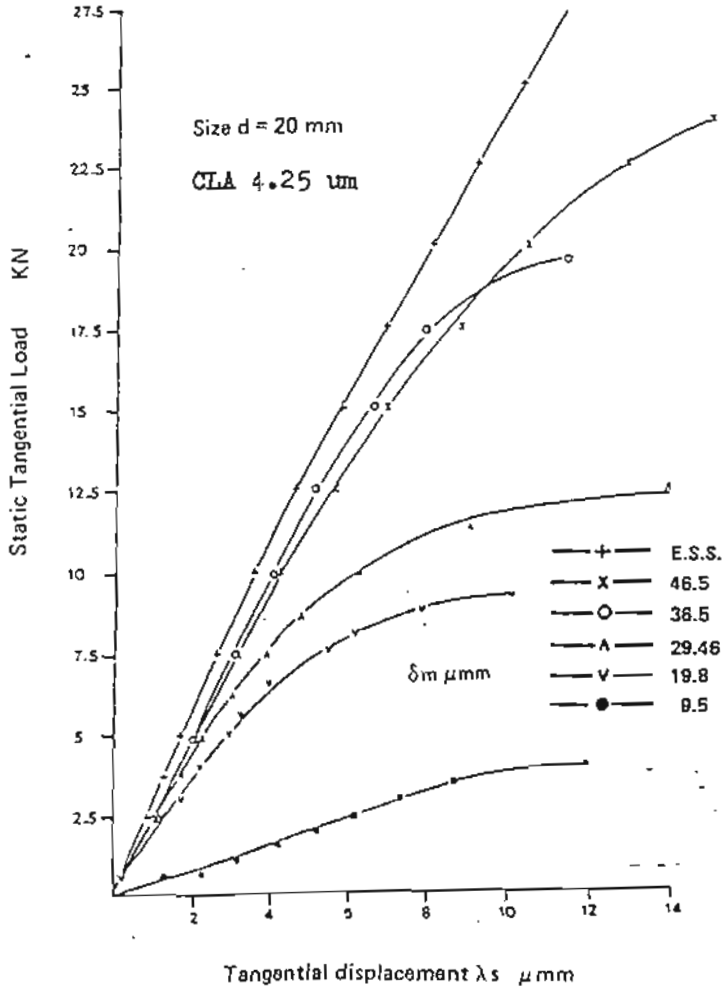

Fig 6 Effect of the interference value on λs of ST51 joints

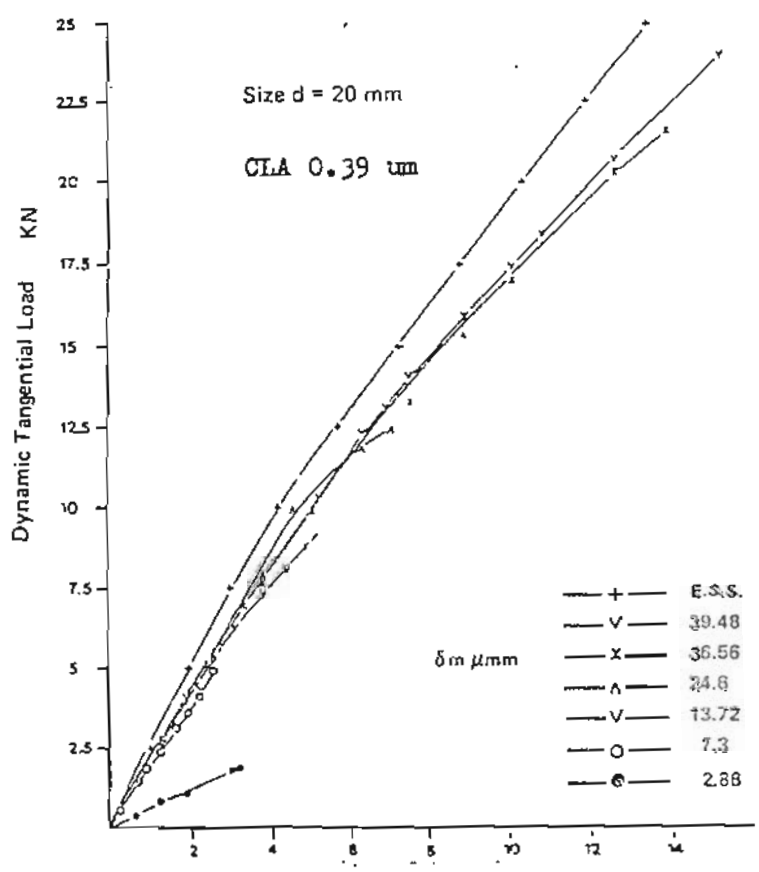

Fig 7 Effect of the interference value on λs of D62 joints

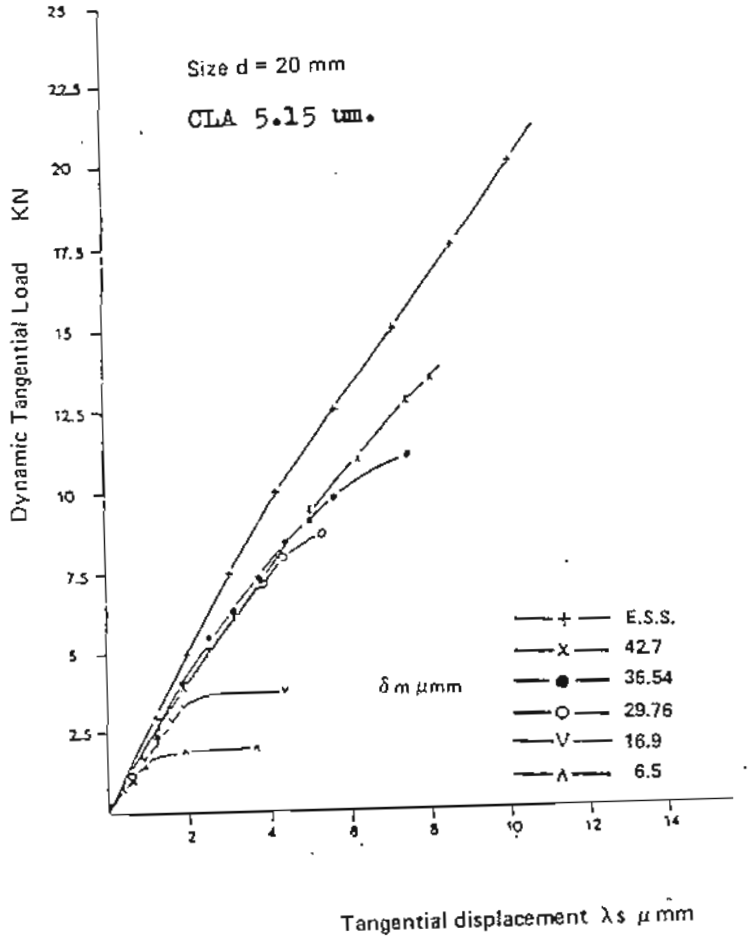

Fig 8 Effect of the interference value on λs of D51 joints

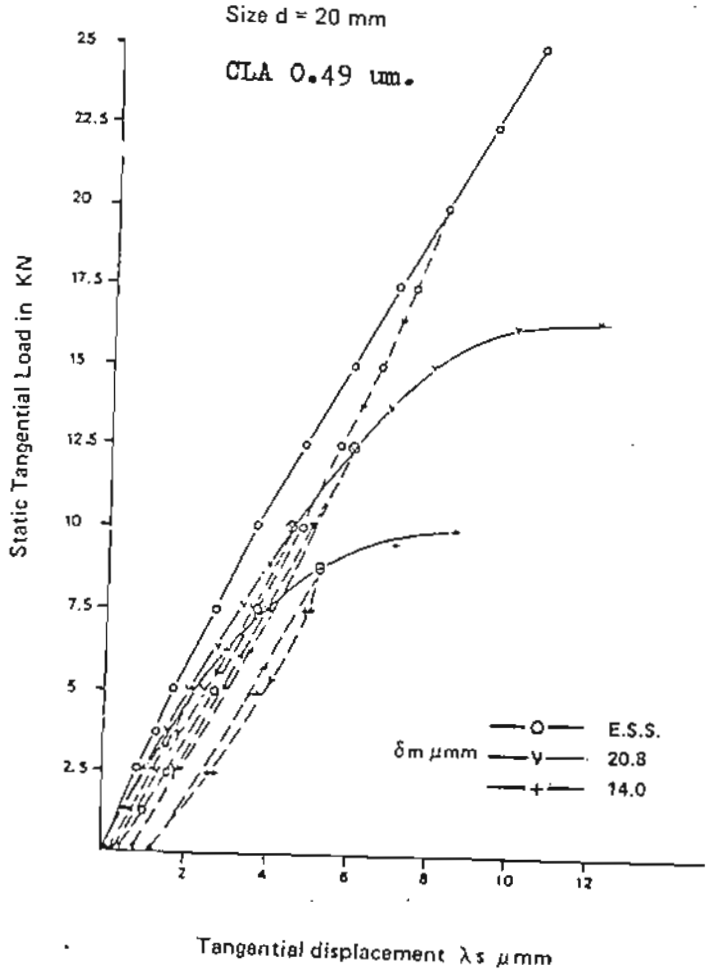

Fig 9 Effect of the interference value on the micro-slip of ST61 joints

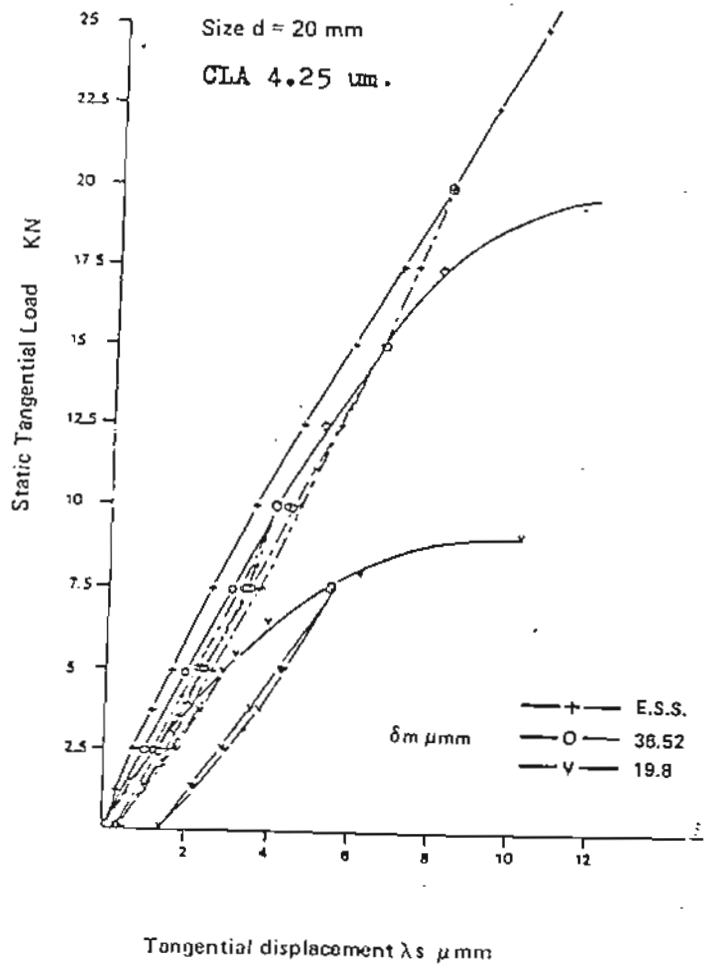

Fig 10 Effect of the interference value on the micro-slip of ST51 joints

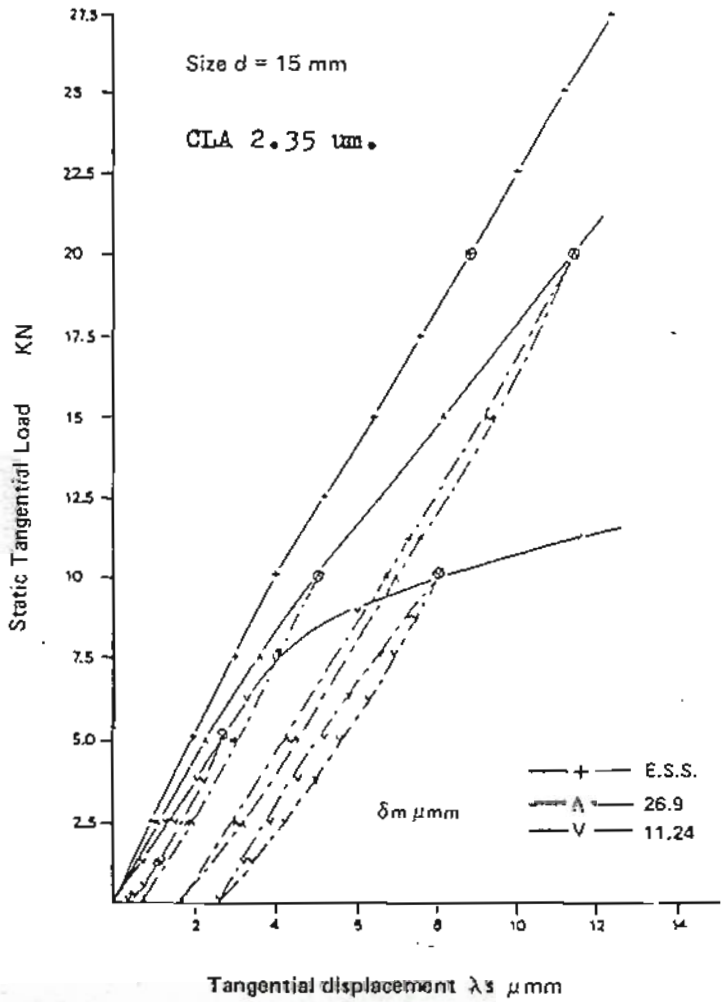

Fig 11 Effect of the interference on the micro-slip of ST31 joints

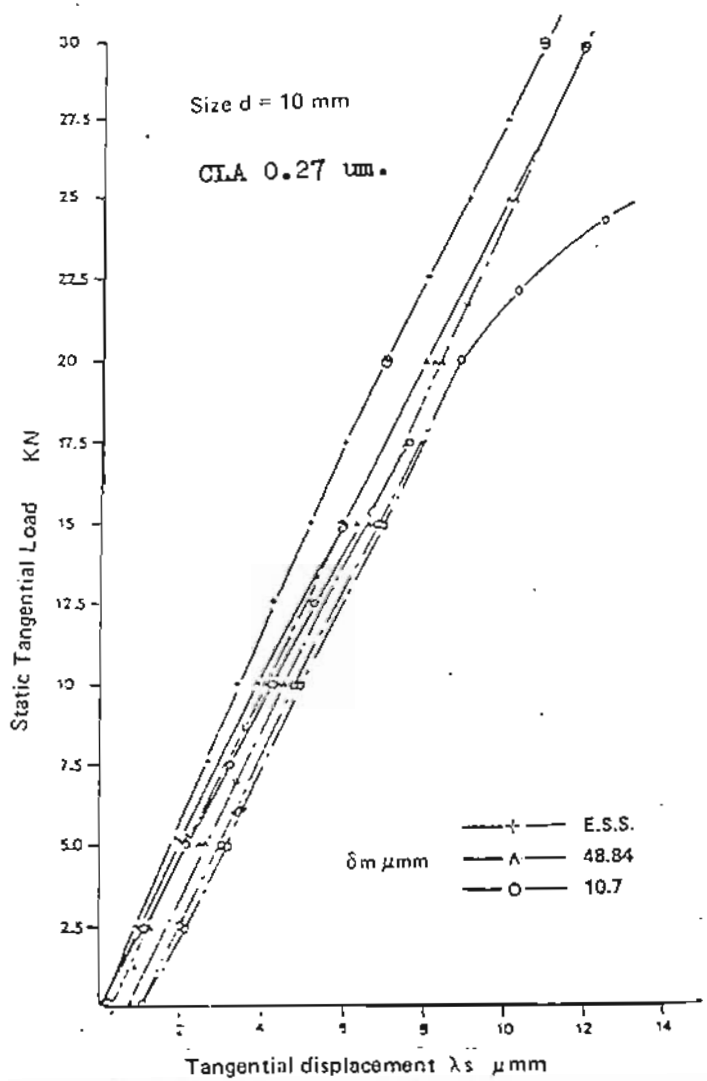

Fig 12 Effect of the interference value on the micro-slip of ST22 Joints

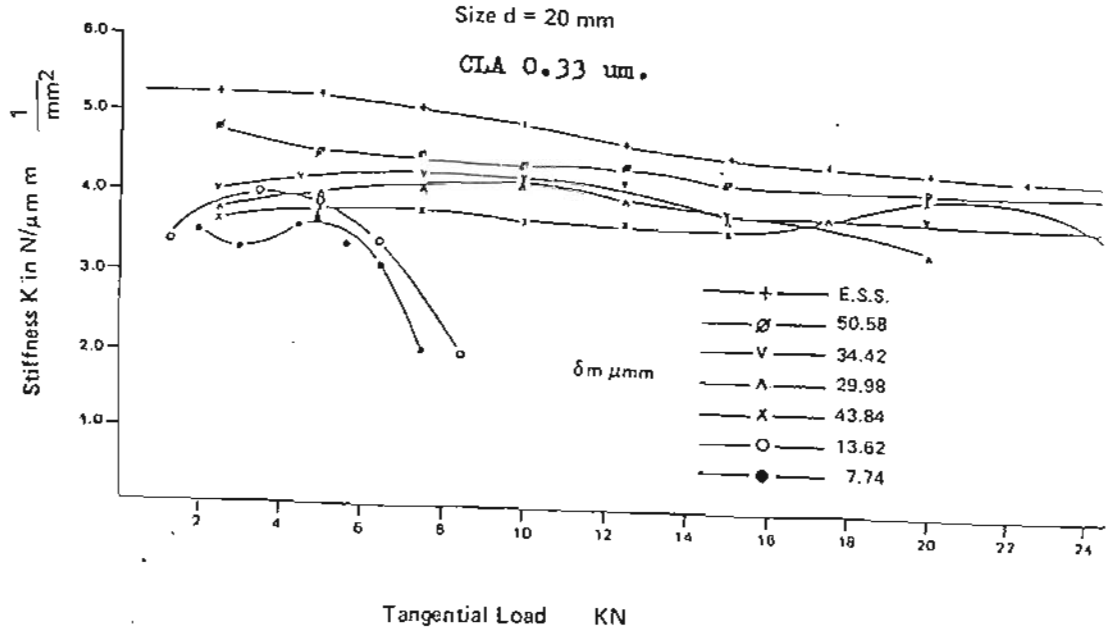

Fig 13 Static stiffness of ST62 joints

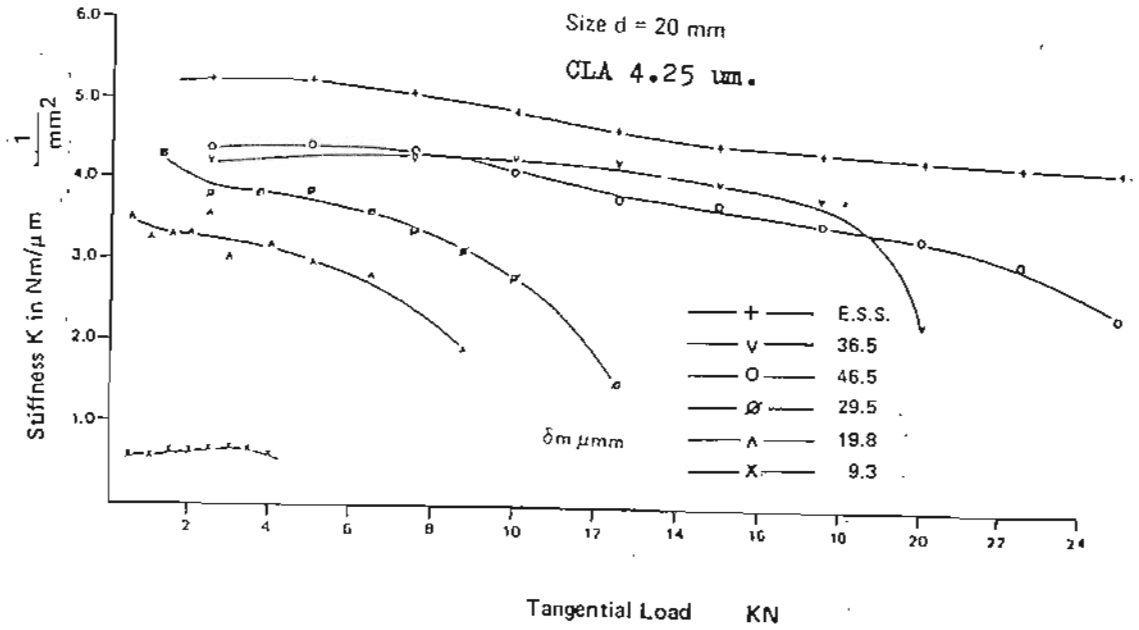

Fig 14 Static stiffness of ST51 joints

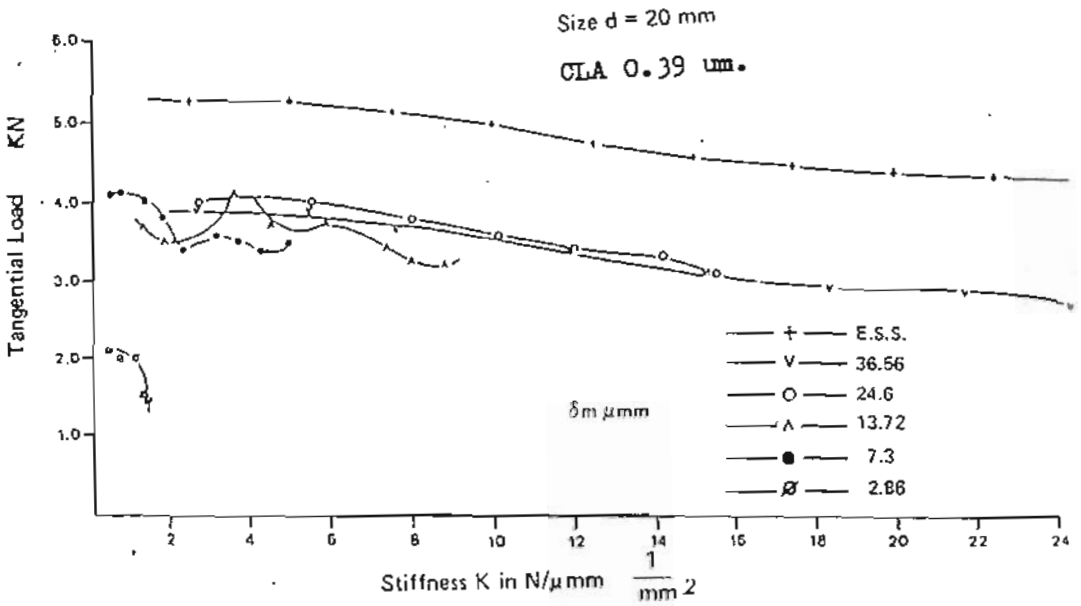

Fig.15 Static stiffness of D62 joints

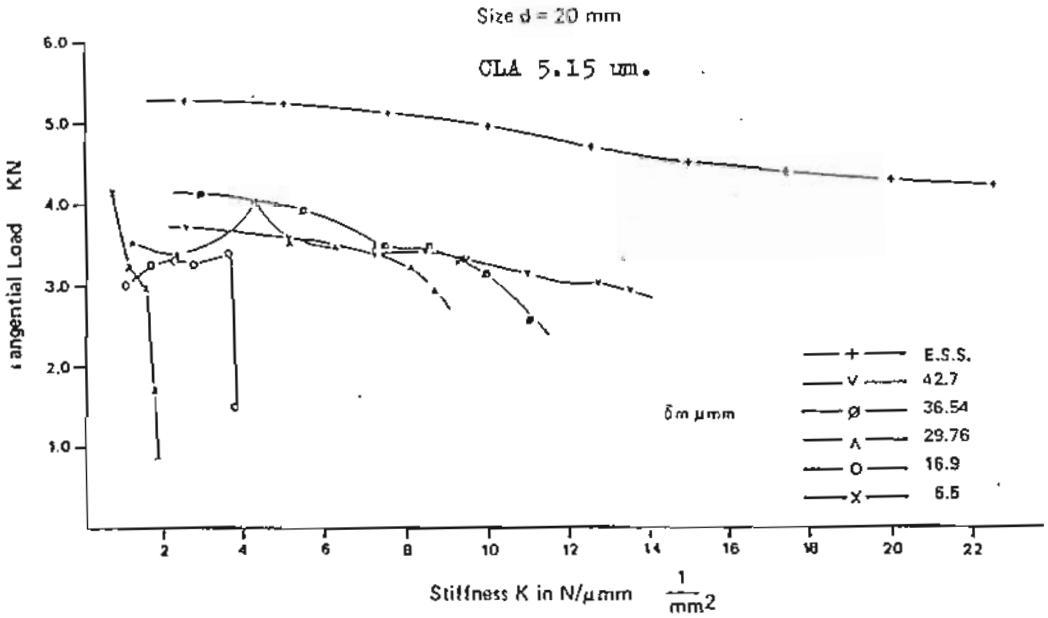

Fig.16 Static stiffness of D51 joints